Electrochemistry and spectroelectrochemistry of substituted tetrabenzotriazaporphine

Yu-Hong Tse, Alok Goel, Mougang Hu, A. B. P. Lever,[1] and C. C. Leznoff

Department of Chemistry, York University, North York, Ont., Canada M3J 1P3

AND

Johan E. Van Lier

Medical Research Council (MRC) Group in the Radiation Sciences, Faculty of Medicine, University of Sherbrooke, Sherbrooke Que., Canada J1H 5N4

Yu-Hong Tse, Alok Goel, Mougang Hu, A. B. P. Lever, C. C. Leznoff, and Johan E. Van Lier. Can. J. Chem. **71**, 742 (1993).

The spectral and electrochemical properties of tetrabenzo[5,10,15]triazaporphine (TBTAP) and its magnesium derivatives having a long alkyl chain attached to the *meso* carbon have been studied. Both metal-free and metallated species show typical metal-free phthalocyanine-like spectra. Two reduction and two oxidation redox couples have been observed. The cation, anion, and dianion species of these porphyrin derivatives have been electrochemically generated and their electronic spectra are recorded.

Yu-Hong Tse, Alok Goel, Mougang Hu, A. B. P. Lever, C. C. Leznoff et Johan E. Van Lier. Can. J. Chem. **71**, 742 (1993).

On a étudié les propriétés spectrales et électrochimiques de la tétrabenzo[5,10,15]triazaporphine (TBTAP) portant une longue chaîne alkyle attaché au carbone *méso* et de ses dérivés contenant du magnésium. Les espèces tant métalliques que non métalliques présentent les spectres caractéristiques des composés ressemblant aux phtalocyanines non-métallisées. On a observé deux couples rédox de réduction et deux d'oxydation. Faisant appel à des méthodes électrochimiques, on a généré les espèces cationiques, anioniques et dianioniques de ces dérivés de la porphyrine et on a enregistré leurs spectres électroniques.

[Traduit par la rédaction]

Introduction

Tetrabenzo[5,10,15]triazaporphine (TBTAP) differs from phthalocyanine (Pc) by a methine group, instead of a nitrogen, at a *meso* position. These unsymmetrical porphyrin derivatives have received relatively less attention than related macrocyclic compounds. During the early development of phthalocyanine chemistry (1, 2) it was shown that reaction of methylmagnesium halide with phthalonitrile yields magnesium tetrabenzotriazaporphine (TBTAPMg). Recently, a variety of TBTAP derivatives (3), substituted at both benzo and *meso* positions, were prepared using a similar procedure. When substituted phthalonitriles are used, inseparable mixtures of regioisomers are obtained. However tetrabenzotriazaporphines derived from unsubstituted phthalonitrile and long-chain alkylmagnesium halide gave only one isomer, which was usually readily soluble in organic solvents. Variations in the alkyl chain length of the Grignard reagent can provide an interesting series of new TBTAP(C$_n$)M derivatives substituted at the *meso* position. ((C$_n$) designates the length of the alkyl chain at the *meso* position.) Unsymmetrical porphyrins have also been used in cancer photodynamic therapy (4). The TBTAP derivatives may provide higher stability and efficiency, in this application, than the generally less stable porphyrin nuclei.

This work reports the syntheses of a series of metal-free, TBTAP(C$_n$)H$_2$, and metallated, TBTAP(C$_n$)M, species with an alkyl chain at the *meso* position. The electrochemical and spectroelectrochemical properties of some of these derivatives will also be reported.

Experimental

Materials

Tetrabutylammonium perchlorate (TBAP; Kodak) was recrystallized from absolute ethanol and dried in a vacuum oven at 50°C for 2 days. 1,2-Dichlorobenzene (DCB, Aldrich) and *N,N*-dimethylformamide (DMF; Aldrich) were used as supplied. Argon gas (Linde) was purified by passage through heated copper filings for electrochemical measurement. Matheson high-purity argon was used to maintain inert atmosphere conditions for syntheses.

Methods

Differential pulse voltammetry was performed with a Princeton Applied Research (PAR) model 174A polarographic analyzer. Cyclic voltammetry was performed with a Pine Instruments RDE-3 potentiostat, and rotating disk electrode studies with a Pine Instruments PIR rotator.

A conventional three-electrode cell was used in electrochemical experiments. A platinum (Pt) disk described by the cross-sectional area of a 27-gauge wire, sealed in glass, was used as the working electrode, a Pt wire as the counter electrode, and a AgCl/Ag wire as the quasi-reference electrode. Potentials were referenced internally to the ferricenium/ferrocene (Fc$^+$/Fc) couple. For the rotating disc study, a Pt disk with an area of 0.44 cm^2 was used as working electrode.

Electronic spectra were recorded with a Guided Wave Inc. model 100-20 optical waveguide spectrum analyser or a Cary model 2400 spectrometer. Spectroelectrochemical data were collected following a published design (5). Note that we used an internal AgCl/Ag electrode and that, in the thin-layer cell, the actual potential of the AgCl/Ag electrode may deviate slightly from its true thermodynamic value. Infrared (ir) spectra were recorded on a Pye Unicam SP1000 infrared spectrophotometer using KBr discs. Nuclear magnetic resonance (nmr) spectra were recorded on a Bruker AM300 nmr spectrometer. The observed splittings of the nmr signals are described as singlets(s), doublets(d), triplets(t), or multiplets(m). Mass spectra (ms) were recorded at 70 eV on a VG Micromass 16F mass spectrometer in the EI mode.
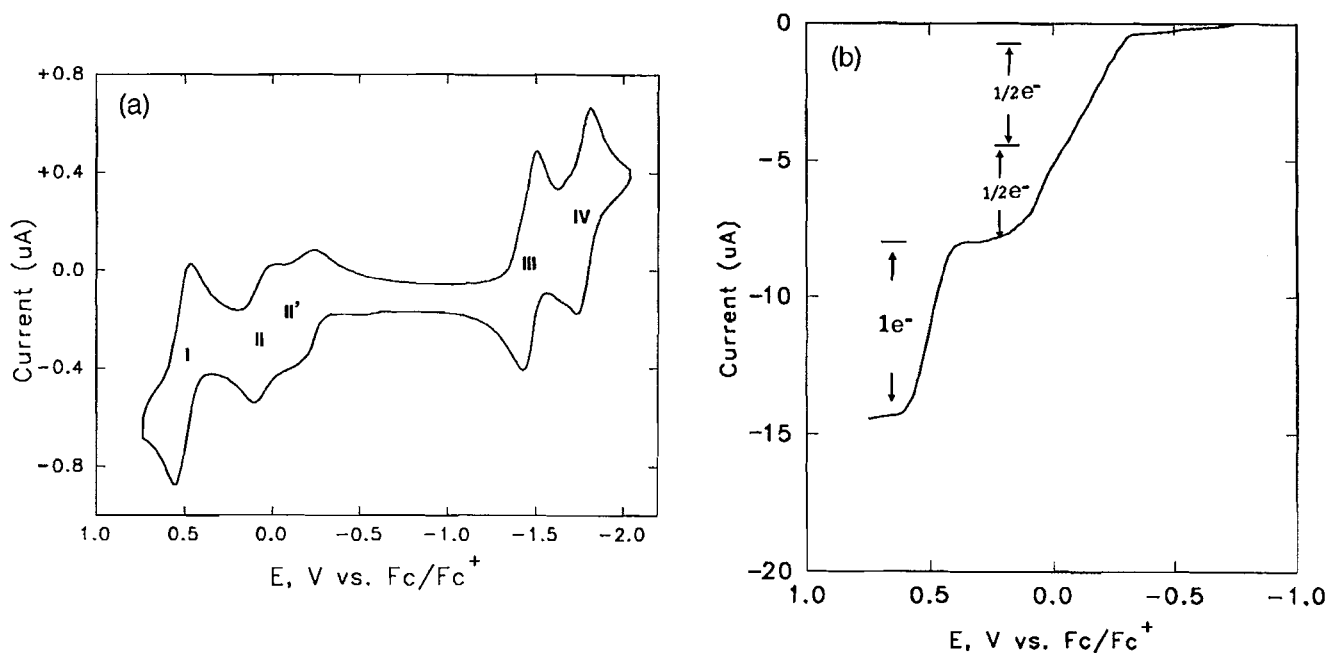
FIG. 1. (a) Cyclic voltammogram for t-NTNTAP(C₁₅)H₂ (14) in DCB (0.15 M TBAP, Pt working electrode, scan rate 100 mV/s). (b) Rotating disc electrode (RDE) study for t-NTNTAP(C₁₅)H₂ (14) in DCB (0.15 M TBAP, Pt disc working electrode, scan rate 10 mV/s, 400 rpm, [t-NTNTAP(C₁₅)H₂] = 2 × 10⁻⁴ M).

Thin-layer chromatography (tlc) was performed using silica gel G as the adsorbent. Flash chromatography was performed using silica gel of particle size 20–45 μm. All reactions were stirred with a magnetic stirrer. Sublimations were generally carried out at 300°C and 0.005 Torr pressure (1 Torr = 133.3 Pa). Microanalyses were performed by Guelph Chemical Laboratories Ltd., Guelph, Ontario.
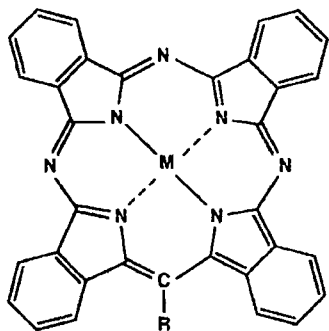
1	M = Mg,	R = $(CH_2)_4CH_3$
2	M = H₂,	R = $(CH_2)_4CH_3$
3	M = Zn,	R = $(CH_2)_4CH_3$
4	M = Mg,	R = $(CH_2)_8CH_3$
5	M = H₂,	R = $(CH_2)_8CH_3$
6	M = Zn,	R = $(CH_2)_8CH_3$
7	M = Mg,	R = $(CH_2)_{12}CH_3$
8	M = H₂,	R = $(CH_2)_{12}CH_3$
9	M = Zn,	R = $(CH_2)_{12}CH_3$
10	M = Mg,	R = $(CH_2)_{16}CH_3$
11	M = H₂,	R = $(CH_2)_{16}CH_3$
12	M = Zn,	R = $(CH_2)_{16}CH_3$

Syntheses

(27-Pentyl-29H,31H-tetrabenzo[b,g,l,q][5,10,15]-triazaporphine) magnesium (1)

Hexylmagnesium chloride (8.0 mL of 2 M solution in diethyl ether, 16 mmol) was added dropwise to a stirred suspension of phthalonitrile (2 g, 15.6 mmol) in dry diethyl ether (10 mL), under an argon atmosphere. The reaction mixture was stirred for 2 h at room temperature. During this time the reaction underwent a colour change from purple to reddish-brown. Ether was removed by passing a stream of argon through the reaction flask for 15 min to obtain a brown residue. This residue was dissolved in distilled quinoline (5 mL) and stirred at 185°C, under argon. After 2 h the reaction mixture underwent a colour change from reddish-brown to green, and tlc analysis (THF–hexane (1:4) as eluant) of this mixture showed the presence of a blue compound, a green compound, and a very mobile purple intermediate. After 24 h the purple intermediate had disappeared and the reaction mixture comprised mainly a blue and a green pigment. The reaction mixture was cooled to room temperature, passed through a silica gel column, and eluted with THF–hexane (1:9). This procedure removed an insoluble blue-black impurity and gave a green fraction. Evaporation of the solvent gave a green semisolid. A solution of this solid was loaded on a silica gel column (flash) and eluted with THF-hexane (1:9) to obtain a green and then a blue fraction. The blue fraction proved to be the magnesium phthalocyanine (by comparison of the uv/vis spectrum with that of an authentic sample). The green fraction was evaporated to obtain a green solid. A solution of this solid was loaded on a gel permeation column (Bio-beads, SX-2, 200–400 mesh) and eluted with THF. This procedure removed a residual trace of yellow impurity. Crystallization from ether–hexane (1:9) gave green needles. After sublimation, under reduced pressure, the sublimate was found to be pure 1 (TBTAP(C₅)Mg) (182 mg, 8% yield); uv/vis (THF) peak λ_{max} (nm) (log ε): 668(5.20), 647(5.00), 615(4,10), 593(4.21), 445(4.43), 400(4.70); ir (cm⁻¹): 2920, 2860, 1490, 1330, 1290, 1170, 1130, 1120, 1090, 720; ¹H nmr (pyridine-d_5) δ: 10.14(m, 2H), 9.80(m, 4H), 9.36(m, 2H), 8.20(m, 8H), 5.40(m, 2H),

TABLE 1. Half-wave potentials (V vs. Fc$^+$/Fc) of metal-free and metallated TBTAP(C$_n$) species

		I	II	II'	III	IV^a
TBTAP(C$_9$)H$_2$^{b} (5)	(i)^c	0.79(ir)	0.41	0.24	−1.42	−1.78
	(ii)	0.76	0.33		−1.41	−1.86
TBTAP(C$_{17}$)H$_2$^{b} (11)	(i)	0.88(ir)	0.47	0.28	−1.36	−1.72
	(ii)	0.84	0.34		−1.37	−1.74
TBuTBTAP(C$_{15}$)H$_2$^{b} (13)	(i)	0.74(ir)	0.32	0.11	−1.49	−1.88
	(ii)	0.71	0.24		−1.51	−1.91
t-NTNTAP(C$_{15}$)H$_2$^{b} (14)	(i)	0.51	0.05	−0.21	−1.48	−1.78
	(ii)	0.46	0.01		−1.44	−1.75
TBTAP(C$_9$)Mg^d (4)	(i)	0.64(ir)	0.14		−1.50	−2.03
	(ii)	0.58	0.12		−1.49	−2.03
TBTAP(C$_{17}$)Mg^d (10)	(i)	0.64(ir)	0.14		−1.48	−2.04
	(ii)	0.58	0.09		−1.48	−2.02

^{a}See text for assignments. Potentials cited for irreversible processes are peak potentials.
^{b}DCB, 0.15 M TBAP.
^{c}(i) cyclic voltammetry at 100 mV/s, (ii) differential pulse voltammetry at 2 mV/s, pulse amplitude 25 mV.
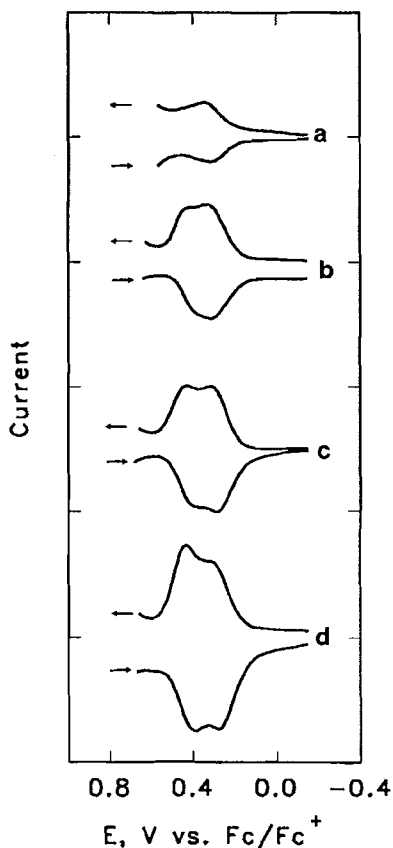^{d}DMF, 0.15 M TBAP.

FIG. 2. Differential pulse voltammogram for TBTAP(C$_9$)H$_2$ in DCB (0.15 M TBAP, Pt electrode). a: 1.8 × 10^{-5} M; b: 6.1 × 10^{-5} M; c: 7.9 × 10^{-5} M; d: 1.8 × 10^{-4} M. Scan rate 2 mV/s, pulse amplitude 25 mV.

2.85(m, 2H), 2.10(m, 2H), 1.58(m, 2H), 1.01(t, J = 7.0 Hz, 3H) ppm; ms m/z: 605(M$^+$, 100), 548(55), 274(28). Anal. calcd. for C$_{38}$H$_{27}$N$_7$Mg: C 75.32, H 4.49, N 16.18; found: C 75.28, H 4.72, N 16.01.

27-Pentyl-29H,31H-tetrabenzo[b,g,l,q][5,10,15]-triazaporphine (2)

Species 1 (61 mg, 0.1 mmol) was dissolved in glacial acetic acid (10 mL), refluxed for 2 h, cooled to room temperature, and centrifuged to obtain a bluish-green precipitate. The precipitate was washed with water and then with methanol. Reprecipitation from a concentrated solution of toluene by methanol gave a bluish-green solid. Crystallization from toluene gave bluish-green needles (44 mg, 75% yield). Residual traces of impurities were sublimed off, under reduced pressure, to obtain a pure sample of 2 (TBTAP(C$_5$)H$_2$); uv/vis (THF) peak λ_{max} (nm) (log ε): 682(5.10), 642(4.89), 616(4.41), 589(3.79), 385(4.33); ir (cm^{-1}): 3440 (br, NH), 2920, 2860, 1500, 1470, 1440, 1340, 1320, 1130, 1120, 1100, 1030, 760, 720; ms m/z: 583(M$^+$, 100), 526(16). Anal. calcd. for C$_{38}$H$_{29}$N$_7$: C 78.19, H 5.01, N 16.80; found: C 78.00, H 4.77, N 16.60.

(27-Pentyl-29H,31H-tetrabenzo[b,g,l,q][5,10,15]-triazaporphine) zinc (3)

To a solution of 2 (29 mg, 0.05 mmol) in 5 mL of dry dimethylformamide(DMF)–toluene (1:1) was added anhydrous zinc acetate (92 mg, 0.5 mmol), and the mixture was refluxed for 20 h (under argon). The reaction mixture was cooled to room temperature and the solvent was evaporated to obtain a green solid. After washing with water and methanol, crystallization from ether gave crystals with a purple reflex. Impurities were removed by sublimation under reduced pressure, affording a residue of pure 3 (TBTAP(C$_5$)Zn) (26 mg, 80% yield) as microcrystals with a purple reflex; uv/vis (THF) peak λ_{max} (nm) (log ε): 668(5.13), 645(4.98), 615(4.22), 591(4.21), 443(4.01), 385(4.50); ir (cm^{-1}): 2920, 2860, 1490, 1410, 1330, 1290, 1170, 1130, 1120, 1100, 780, 720; ms m/z: 645 (M$^+$, 100), 588(39), 294(23). Anal. calcd. for C$_{38}$H$_{27}$N$_7$Zn: C 70.54, H 4.18, N 15.15; found: C 70.28, H 4.00, N 15.00.

(27-Nonyl-29H,31H-tetrabenzo[b,g,l,q][5,10,15]-triazaporphine) magnesium (4)

Decylmagnesium bromide (7.8 mL of 1 M solution in diethyl ether, 7.8 mmol) was added dropwise to a stirred suspension of phthalonitrile (1 g, 7.8 mmol) in dry diethyl ether (5 mL), under an argon atmosphere. The reaction mixture was stirred for 2 h at room temperature. During this time, the reaction underwent a colour change from purple to reddish-brown. Ether was removed by passing a stream of argon through the reaction flask for 15 min to obtain a brown residue that was dissolved in distilled quinoline (5 mL) and stirred at 120°C, under argon. After 2 h the reaction
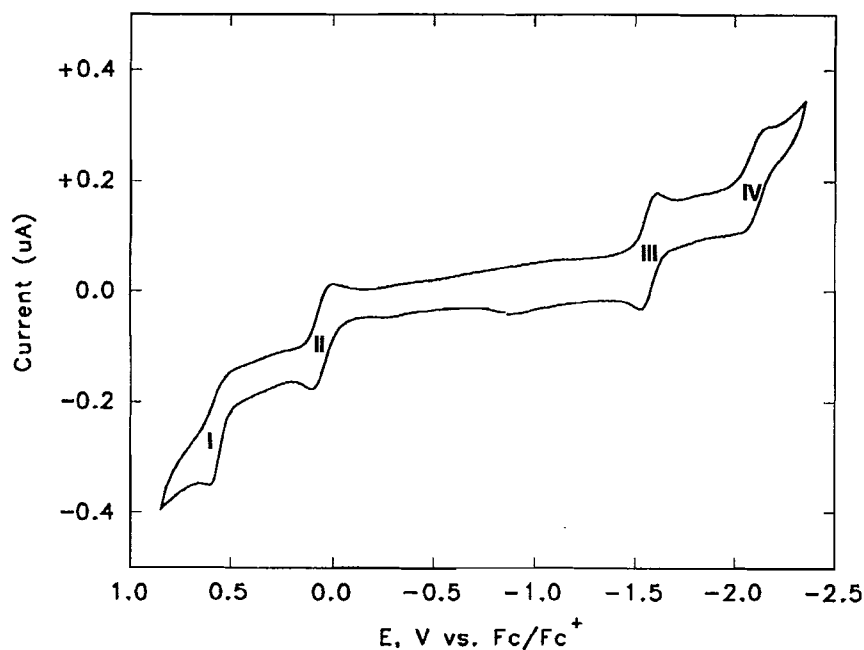
FIG. 3. Cyclic voltammogram for TBTAP(C₉)Mg in DMF (0.15 M TBAP, Pt working electrode, scan rate 100 mV/s).

mixture underwent a colour change from reddish-brown to green, and tlc analysis (pyridine–hexane (1:4) as eluant) of this mixture showed the presence of a blue compound, a green compound, and a very mobile purple intermediate. After 18 h the purple intermediate had disappeared and the reaction mixture comprised mainly a blue and a green pigment. The reaction mixture was cooled to room temperature, passed through a silica gel column, and eluted with ether–hexane (1:1). This procedure removed an insoluble blue-black impurity and gave a green fraction. Evaporation of the solvent gave a green semisolid. A solution of this solid was loaded on a silica gel column (flash) and eluted with pyridine–hexane (1:4) to obtain a green and then a blue fraction. The green fraction was evaporated to obtain a green solid. Crystallization from ether–hexane (1:9) gave pure **4** (TBTAP(C₉)Mg) as green needles (100 mg, 8% yield); uv/vis (THF) peak λ_{max} (nm) (log ε): 668(5.22), 647(5.06), 615(4.18), 593(4.25), 445(4.48), 400(4.74); ir (cm⁻¹): 2920, 2860, 1490, 1330, 1290, 1170, 1130, 1120, 1090, 720; ¹H nmr (pyridine-d_5) δ: 10.14 (m, 2H), 9.80 (m, 4H), 9.42 (d, J = 7.5 Hz, 2H), 8.22 (m, 8H), 5.46 (m, 2H), 2.92 (m, 2H), 2.22 (m, 2H), 1.62 (m, 2H), 1.60–1.20 (m, 8H), 0.91 (t, J = 7.0 Hz, 3H) ppm; ms m/z: 661 (M⁺, 100), 548(41), 535(9).

27-Nonyl-29H,31H-tetrabenzo[b,g,l,q][5,10,15]-triazaporphine (5)

Species **4** (75 mg, 0.11 mmol) was dissolved in glacial acetic acid (10 mL), refluxed for 2 h, cooled to room temperature, and centrifuged to obtain a bluish-green precipitate. The precipitate was washed with water and then with methanol. Reprecipitation from a concentrated solution of toluene by methanol gave a bluish-green solid. Crystallization from toluene gave bluish-green needles (55 mg, 78% yield). Residual trace impurities were sublimed off, under reduced pressure, to obtain pure **5** (TBTAP(C₉)H₂); uv/vis (THF) peak λ_{max} (nm) (log ε): 682(5.13), 642(4.93), 616(4.40), 589(3.80), 385(4.38); ir (cm⁻¹): 3440 (br, NH), 2920, 2860, 1500, 1470, 1440, 1340, 1320, 1130, 1120, 1100, 1030, 760, 720; ms m/z: 639 (M⁺, 80), 473 (38). Anal. calcd. for C₄₂H₃₇N₇: C 78.85, H 5.83, N 15.32; found: C 78.50, H 6.23, N 14.95.

(27-Nonyl-29H,31H-tetrabenzo[b,g,l,q][5,10,15]-triazaporphine) zinc (6)

To a solution of **5** (25.5 mg, 0.04 mmol) in 5 mL of dry dimethylformamide (DMF)–toluene (1:1) was added anhydrous

zinc acetate (73.6 mg, 0.4 mmol), and the mixture was refluxed for 20 h (under argon). The reaction mixture was cooled to room temperature and the solvent was evaporated to obtain a green solid. After washing with water and methanol, crystallization from ether gave crystals with a purple reflex. Sublimation under reduced pressure afforded a sublimate of pure **6** (TBTAP(C₉)Zn) (24 mg, 85% yield) as microcrystals with a purple reflex; uv/vis (THF) peak λ_{max} (nm) (log ε): 668(5.15), 645(4.98), 615(4.23), 591(4.20), 443(3.98), 385(4.58); ir (cm⁻¹): 2920, 2860, 1490, 1410, 1330, 1290, 1170, 1130, 1120, 1100, 780, 720; ms m/z: 703(M⁺, 71), 576(100), 471(34), 288(33).

(27-Tridecyl-29H,31H-tetrabenzo[b,g,l,q][5,10,15]-triazaporphine) magnesium (7)

Tetradecylmagnesium chloride (7.8 mL of 1 M solution in THF, 7.8 mmol) was added dropwise to a stirred suspension of phthalonitrile (1 g, 7.8 mmol) in freshly distilled THF (5 mL), under an argon atmosphere. The reaction mixture turned purple immediately. The reaction mixture was stirred for a further 2 h at room temperature. During this time, the reaction underwent a colour change from purple to reddish-brown. Tetrahydrofuran was removed by passing a stream of argon through the reaction flask for 15 min to obtain a dark brown residue, which was dissolved in distilled quinoline (3 mL) and the mixture stirred at 120°C, under an argon atmosphere. After 0.5 h the reaction mixture underwent a colour change from reddish-brown to dark green, and tlc analysis (pyridine–hexane (1:4) as eluant) of this mixture showed the presence of a blue compound, a green compound, and a purple intermediate. After 18 h the purple intermediate was still present. Hence, the temperature was raised to 180°C and the mixture was refluxed for a further 24 h. The reaction mixture was cooled to room temperature and loaded on a short silica gel column (flash). The column was eluted with pyridine–hexane (1:4) and a green fraction was collected. The solvent was evaporated to obtain a green oil. This oil was loaded on another silica gel column (flash) and again eluted with pyridine–hexane (1:4). This chromatographic procedure afforded separation of the required product from the phthalocyanine by-product. Reprecipitation from a concentrated solution of THF (1 mL) by methanol (9 mL) gave crude **7** (TBTAP(C₁₃)Mg) (47 mg, 3% yield). After sublimation, under
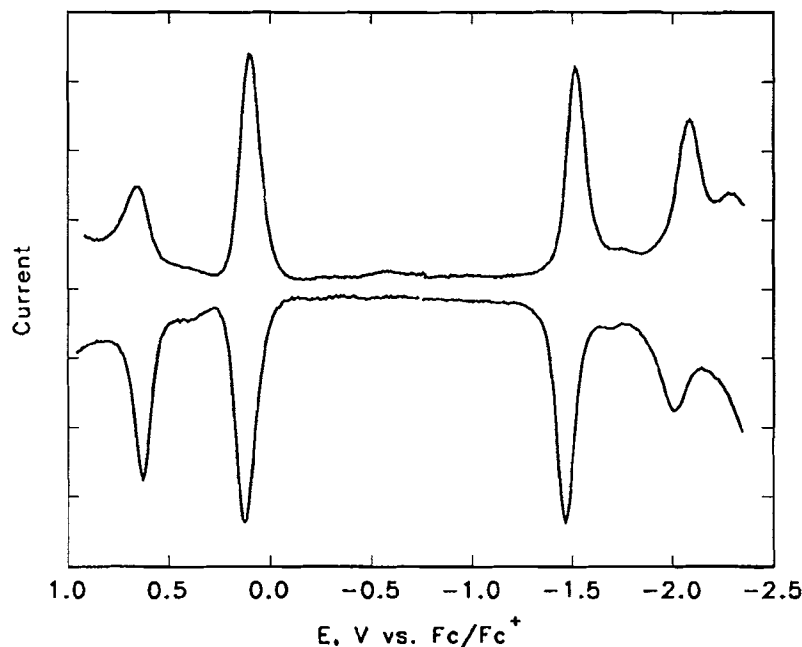
FIG. 4. Differential pulse voltammogram for TBTAP(C₉)Mg in DMF (0.15 M TBAP, Pt electrode). Scan rate 2 mV/s, pulse amplitude 25 mV.
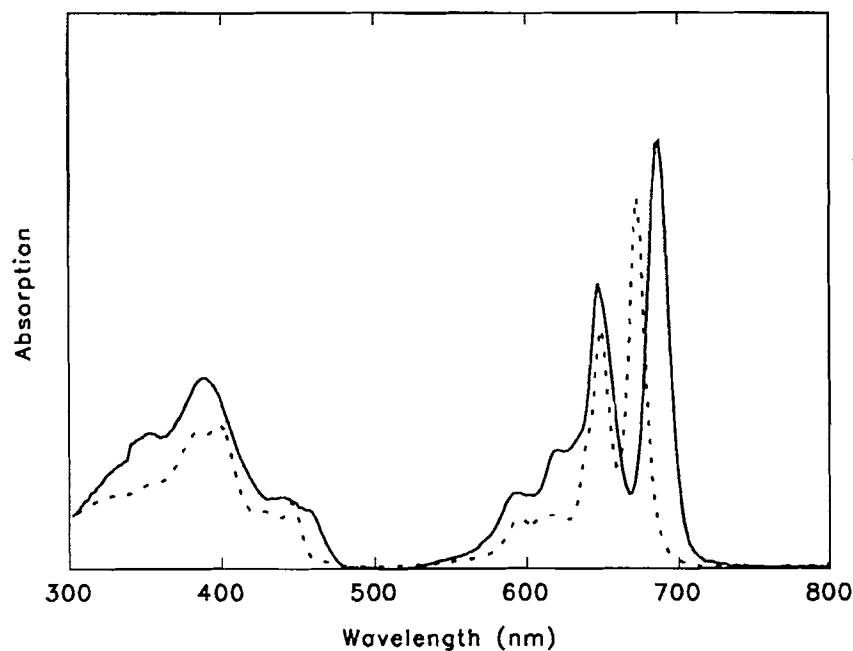

FIG. 5. Absorption spectra of TBTAP(-2)(C₉)H₂ (5) (solid line) in DCB and TBTAP(C₉)Mg (4) (dotted line) in DMF.

reduced pressure, the sublimate had a purple reflex and was found to be the pure 7; uv/vis (THF) peak λ_{max} (nm) (log ε): 668(5.25), 647(5.03), 615(4.09), 593(4.20), 445(4.62), 400(4.74); ir (cm⁻¹): 2920, 2860, 1490, 1330, 1290, 1170, 1130, 1120, 1090, 720; ¹H nmr (pyridine-d_5) δ: 10.14 (m, 2H), 9.80 (m, 4H), 9.42 (d, J = 7.3 Hz, 2H), 8.22 (m, 8H), 5.46 (m, 2H), 2.92 (m, 2H), 2.22 (m, 2H), 1.64 (m, 2H), 1.42–1.25 (m, 16H), 0.91 (t, J = 7.0 Hz, 3H) ppm; ms m/z: 717(M⁺, 100), 548(44), 535(18). Anal. calcd. for $C_{46}H_{43}N_7Mg$: C 76.93, H 6.03, N 13.65; found: C 76.74, H 6.22, N 13.44.

27-Tridecyl-29H,31H-tetrabenzo[b,g,l,q]-[5,10,15]-triazaporphine (8)

Species 7 (40 mg, 0.056 mmol) was dissolved in glacial acetic acid (5 mL), refluxed for 2 h, cooled to room temperature, and centrifuged to obtain a bluish-green precipitate. The precipitate was washed with water and then with methanol until the washings were colourless. Reprecipitation from a concentrated solution of toluene by methanol gave a bluish-green solid. Crystallization from toluene gave needles with a purple reflex (28 mg, 72% yield). After sublimation under reduced pressure, the residue was found to be

TABLE 2. Observed maxima in the absorption spectra of TBTAP(-2)(C_n) species[a]

Complex	λ_{max}(nm) (log ε)				
TBTAP(C_9)H$_2$ (5)[b]	687(4.81)	647(4.62)	621(4.21)	593(4.02)	388(4.48)
TBTAP(C_{17})H$_2$ (11)[b]	686(4.69)	647(4.49)	619(4.11)	593(3.90)	386(4.49)
TBTAP(C_9)Mg (4)[c]	672(5.13)	648(4.95)	619(4.28)	595(4.26)	399(4.73)
				355(4.48)	327(4.42)
TBuTBTAP(C_{15})H$_2$ (13)[b]	693(5.19)	653(4.99)	625(4.62)	598(4.42)	390(4.87)
t-NTNTAP(C_{15})H$_2$ (14)[b]	785(5.31)	753(5.10)	718(4.63)	683(4.56)	376(4.80)
TBTAP(C_{17})Mg (10)[c]	672(5.26)	648(5.05)	617(4.35)	595(4.32)	398(4.80)
				353(4.53)	327(4.46)

[a]The solvent was that used for the electrochemistry experiments and therefore contains 0.15 M TBAP.
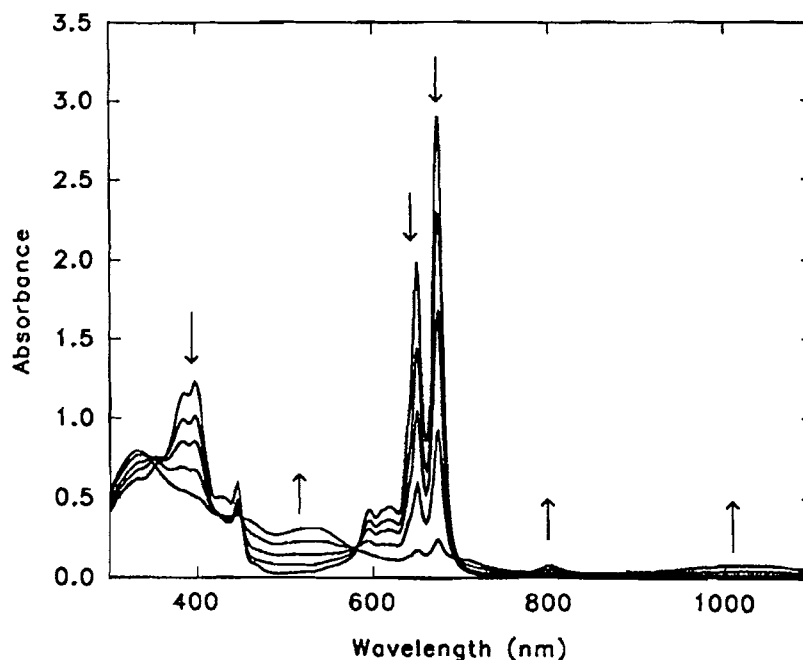[b]Solvent, DCB.
[c]Solvent, DMF.

FIG. 6. Spectroscopic changes accompanying the controlled potential oxidation of TBTAP(-2)(C_9)Mg (4) (8.6 × 10^{-4} M) in DMF (0.15 M TBAP). The first (top) spectrum is the starting material, unpolarized. Successive spectra are equilibrium spectra obtained with the electrode polarized at 0.45, 0.50, 0.55, and 0.575 V vs. AgCl/Ag.

the pure 8 (TBTAP(C_{13})H$_2$); uv/vis (THF) peak λ_{max} (nm) (log ε): 682(5.15), 642(4.94), 616(4.45), 589(3.82), 385(4.47); ir (cm^{-1}): 3440 (bd, NH), 2920, 2860, 1500, 1470, 1440, 1340, 1320, 1130, 1120, 1100, 1030, 760, 720; ms m/z: 695 (M$^+$, 100), 526 (10). Anal. calcd. for $C_{46}H_{45}N_7$: C 79.39, H 6.52, N 14.09; found: C 79.42, H 6.34, N 14.39.

(27-Tridecyl-29H,31H-tetrabenzo[b,g,l,q][5,10,15]-
triazaporphine) zinc (9)

Anhydrous zinc acetate (73.6 mg, 0.4 mmol) was added to a solution of 8 (17.35 mg, 0.025 mmol) in 5 mL of dry DMF–toluene (1:1) and the mixture refluxed for 24 h (under argon). The reaction mixture was cooled to room temperature and the solvent evaporated to obtain a green solid. After washing with water and methanol, crystallization from ether gave dark blue crystals. After sublimation under reduced pressure, the residue was found to be the pure 9 (TBTAP(C_{13})Zn), (12 mg, 63% yield); uv/vis (THF) peak λ_{max} (nm) (log ε): 668(5.13), 645(5.00), 615(4.28), 591(4.25), 443(4.21), 385(4.63); ir (cm^{-1}): 2920, 2860, 1490, 1410, 1330, 1290, 1170, 1130, 1120, 1100, 780, 720; ms m/z: 758(M$^+$, 100), 588(41), 575(14), 294(14).

(27-Heptadecyl-29H,31H-tetrabenzo[b,g,l,q][5,10,15]-
triazaporphine) magnesium (10)

Octadecylmagnesium chloride (7.8 mL of 1 M solution in THF, 7.8 mmol) was added dropwise to a stirred suspension of phthalonitrile (1 g, 7.8 mmol) in freshly distilled THF (5 mL), under an argon atmosphere. The reaction mixture was stirred for 2 h at room temperature. Tetrahydrofuran was removed by passing a stream of argon through the reaction flask. Distilled quinoline (5 mL) was added and the mixture was stirred at 140°C, under argon, for 18 h. A tlc analysis (THF–hexane (1:1) as eluant) showed a very mobile green spot for the required product along with some brown impurities. The reaction mixture was cooled to room temperature, passed through a silica gel column, and eluted with THF–hexane (1:1). This procedure removed an insoluble blue-black impurity and gave a green fraction. A tlc analysis (pyridine–hexane (1:4) as eluant) of this fraction showed a green spot (R_f 0.9) for the required magnesium tetrabenzotriazaporphine and a blue spot (R_f 0.25) for the magnesium phthalocyanine by-product. The solvent was evaporated and the residue loaded onto a silica gel column (flash) and eluted with pyridine–hexane (1:9). This chro-
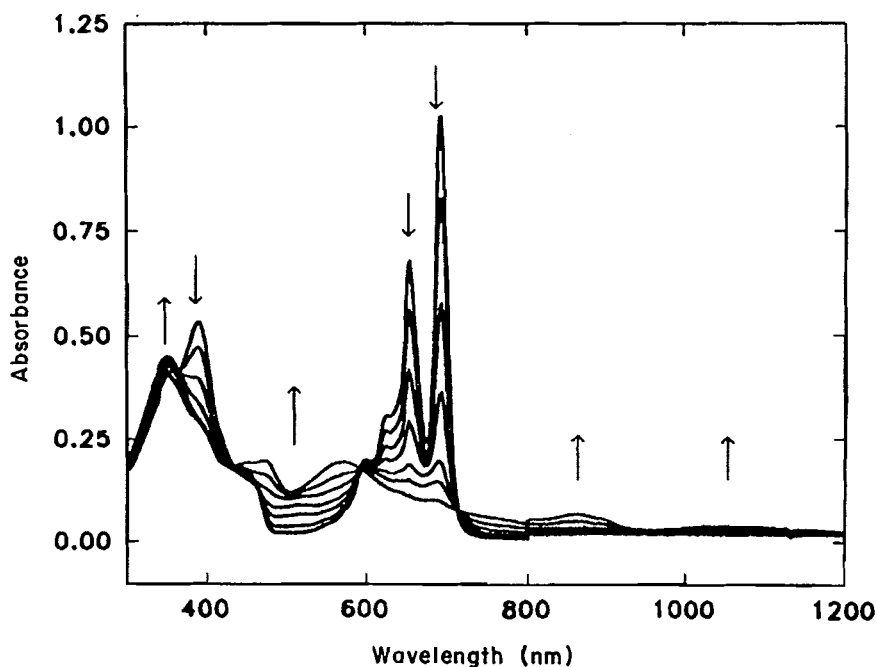
FIG. 7. Spectroscopic changes accompanying the controlled potential oxidation of TBuTBTAP(-2)(C$_{15}$)H$_2$ (13) (2.7 × 10^{-4} M) in DCB (0.15 M TBAP). The first (top) spectrum is the starting material, unpolarized. Successive spectra are equilibrium spectra obtained with the electrode polarized at 0.575, 0.60, 0.625, 0.65, 0.675, and 0.70 V vs. AgCl/Ag (see experimental section for additional comment).

TABLE 3. Observed maxima in the absorption of [TBTAP(-1)(C$_n$)]$^+$ cations^a

Complex	λ_{max}(nm)					
TBTAP(C$_9$)H$_2$ (5)^b	1019	859	684	570	472	345
TBTAP(C$_9$)Mg (4)^{c,d}	1023	800	678	530	449	330
TBuTBTAP(C$_{15}$)H$_2$ (13)^b	1070	856	683	558	470	342

^{a}The solvent was that used for the electrochemistry experiments and therefore contains 0.15 M TBAP. The product is an equilibrium mixture of mononuclear and binuclear species; the extinction coefficients have therefore not been included.
^{b}DCB.
^{c}DMF.
^{d}Incomplete oxidation of parent species.

matographic procedure afforded separation of the required 10 (TBTAP(C$_{17}$)Mg) from the phthalocyanine by-product. Crystallization from THF–methanol (1:1) gave 10 as needles with a purple reflex (86 mg, 6% yield); uv/vis(THF) peak λ_{max} (nm) (log ε): 668(5.24), 647(5.06), 615(4.09), 593(4.20), 445(4.60), 400(4.71); ir (cm^{-1}): 2920, 2860, 1490, 1330, 1290, 1170, 1130, 1120, 1090, 720; ^{1}H nmr (pyridine-d_5) δ: 10.14(m, 2H), 9.8(m, 4H), 9.42(d, J = 7.9 Hz, 2H), 8.22(m, 2H), 5.46(m, 2H), 2.92(m, 2H), 2.21(m, 2H), 1.62(m, 2H), 1.42–1.23(m, 24H), 0.84(t, J = 7.0 Hz, 3H) ppm; ms m/z: 774(M$^+$, 100), 548(56), 535(20).

27-Heptadecyl-29H,31H-tetrabenzo[b,g,l,q][5,10,15]-triazaporphine (11)

Compound 10 (86 mg, 0.11 mmol) was dissolved in glacial acetic acid (5 mL), refluxed for 2 h, cooled to room temperature, and centrifuged to obtain a bluish-green precipitate. The precipitate was washed with water and then with methanol until the washings were colourless. Reprecipitation from a concentrated solution of toluene by methanol gave a bluish-green solid. Crystallization from toluene gave plates with a purple reflex (60 mg, 70% yield). After sublimation under reduced pressure, the residue was found to

be the pure 11 (TBTAP(C$_{17}$)H$_2$); uv/vis (THF) peak λ_{max} (nm) (log ε): 682(5.28), 642(5.09), 616(4.61), 589(3.71), 385(4.46); ir (cm^{-1}): 3260 (br, NH), 2920, 2860, 1500, 1470, 1440, 1340, 1320, 1130, 1120, 1100, 1030, 760, 720; ms m/z: 751(M$^+$, 100), 526(9).

(27-Heptadecyl-29H,31H-tetrabenzo[b,g,l,q][5,10,15]-triazaporphine) zinc (12)

To a solution of 11 (30 mg, 0.04 mmol) in 5 mL of dry DMF–toluene (1:1) was added anhydrous zinc acetate (73.6 mg, 0.4 mmol), and the mixture was refluxed for 24 h (under argon). The reaction mixture was cooled to room temperature and the solvent evaporated to obtain a green solid. After washing with water and methanol, crystallization from ether gave a bluish-green solid. Further purification by flash chromatography, using a solvent system of pyridine–hexane (1:9), and sublimation under reduced pressure gave a residue with a purple reflex. It was found to be the pure 12 (TBTAP(C$_{17}$)Zn) (20 mg, 61% yield); uv/vis (THF) peak λ_{max} (nm) (log ε): 668(5.23), 645(5.05), 615(4.34), 591(4.29), 443(4.16), 385(4.66); ir (cm^{-1}): 2920, 2860, 1490, 1410, 1330, 1290, 1170, 1130, 1120, 1100, 780, 720; ms m/z: 814 (M$^+$, 100),
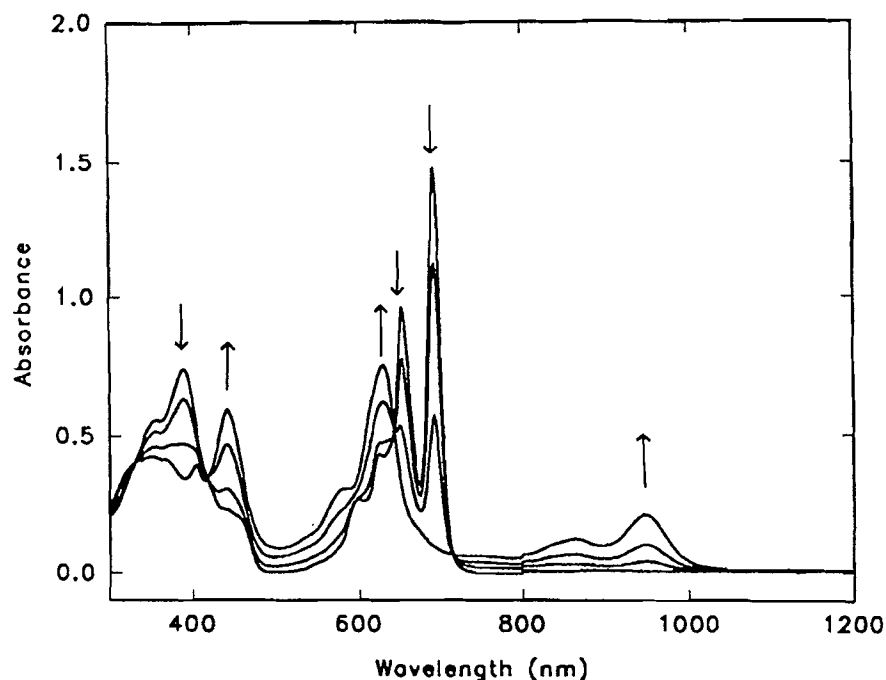
Fig. 8. Spectroscopic changes accompanying the controlled potential reduction of TBuTBTAP(-2)(C$_{15}$)H$_2$ (**13**) (3.8 × 10^{-4} M) in DCB (0.15 M TBAP). The first (top) spectrum is the starting material, unpolarized. Successive spectra are equilibrium spectra obtained with the electrode polarized at −1.25, −1.275, and −1.30 V vs. AgCl/Ag.

TABLE 4. Observed maxima in the absorption spectra of TBTAP(C$_n$) anion radicals

Complex	λ_{max}(nm) (log ε)			
[TBTAP(-3)(C$_9$)H$_2$]$^-$ (**5**$^-$)[b]	948(4.38)	864(4.08)	630(4.90)	583(sh)
		442(4.83)	404(4.61)	351(4.61)
[TBTAP(-4)(C$_9$)H$_2$]$^{2-}$ (**5**$^{2-}$)[b]	619(sh)	530(4.96)	338(4.55)	
[TBTAP(-3)(C$_9$)Mg]$^-$ (**4**$^-$)[c]	860(4.23)	754(3.89)	631(4.77)	534(sh)
	449(4.78)	401(4.46)	372(4.48)	319(4.41)
[TBuTBTAP(-3)(C$_{15}$)H$_2$]$^-$ (**13**$^-$)[b]	943(4.51)	862(4.27)	630(5.06)	579(sh)
	443(4.96)	403(4.77)	348(4.81)	
[TBuTBTAP(-4)(C$_{15}$)H$_2$]$^{2-}$ (**13**$^{2-}$)[b]	623(sh)	528(5.16)	340(4.74)	

[a]The solvent was that used for the electrochemistry experiments and contains 0.15 M TBAP.
[b]DCB.
[c]DMF.
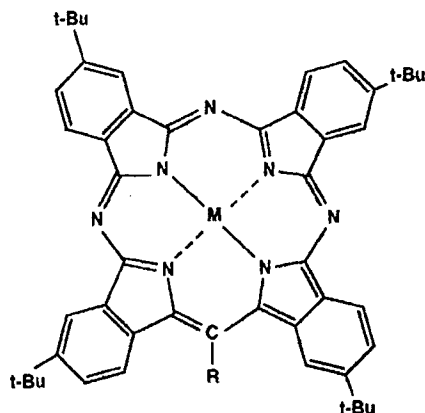
13 M = H$_2$, R = (CH$_2$)$_{14}$CH$_3$

589(47), 575(29), 294(21). Anal. calcd. for C$_{50}$H$_{51}$H$_{17}$Zn: C 73.65, H 6.30, N 12.02; found: C 73.60, H 6.43, N 12.55.

2,9,16,23-Tetrakis(2,2-dimethylethyl)-27-pentadecyl-29H,31H-tetrabenzo[b,g,l,q][5,10,15]triazaporphine (TBuTBTAP(C$_{15}$)H$_2$) (13) and 2,11,20,29-tetrakis(2,2-dimethylethyl)-34-pentadecyl-37H,39H-tetranaphtho-[2,3-b:2',3'-g:2'',3''-l-2''',3'''-q][5,10,15]triazaporphine (t-NTNTAP(C$_{15}$)H$_2$) (14) were synthesized as previously described (3).

Results and discussion

A. Syntheses

Reaction of phthalonitrile with a variety of Grignard reagents led to the formation of magnesium tetrabenzotriazaporphines, TBTAP(C$_n$)Mg, along with some magnesium phthalocyanine (MgPc) by-product. Magnesium tetrabenzotriazaporphines could be separated from the magnesium phthalocyanine by using flash chromatography. Sometimes
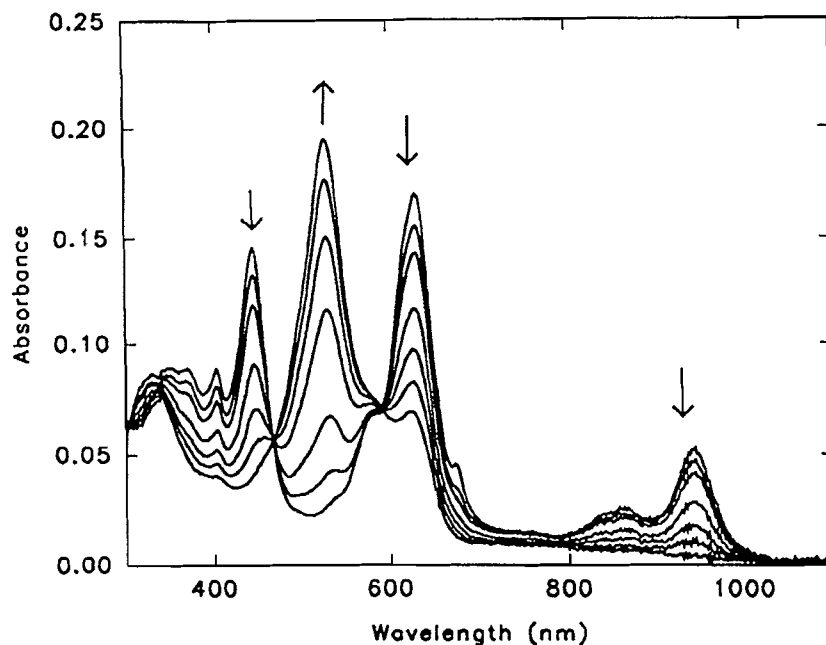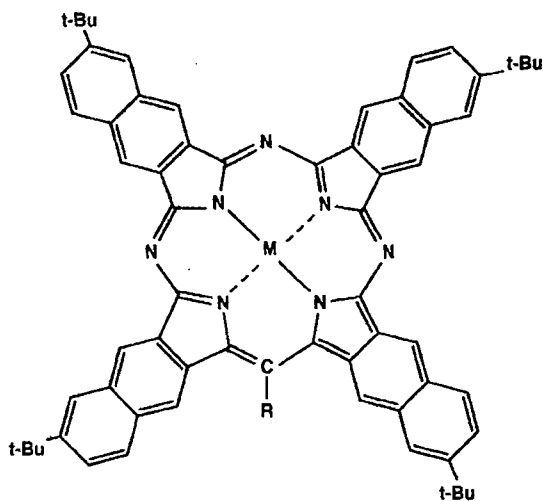
FIG. 9. Spectroscopic changes accompanying the controlled potential reduction of $[\text{TBTAP}(-3)(\text{C}_9)\text{H}_2]^-$ (**5**⁻) (8.8×10^{-5} M) in DCB (0.15 M TBAP). These spectra were obtained as a series by polarizing the electrode from -1.30 to -1.45 V vs. AgCl/Ag in 0.025 V steps (see experimental section for further comment).

14 $\quad$ M = H$_2$, $\quad$ R = (CH$_2$)$_{14}$CH$_3$

it was necessary to filter the product mixture through a normal silica gel column to remove insoluble impurities, before performing the flash chromatography. Magnesium TBTAP species were further purified by crystallization from ether–hexane or tetrahydrofuran (THF)–methanol, and sublimation under reduced pressure. The sublimate was usually a brown impurity and the residue the required pure TBTAP(C$_n$)Mg.

Magnesium tetrabenzotriazaporphines could be demetallated by refluxing in glacial acetic acid. Metal-free tetrabenzotriazaporphines (TBTAP(C$_n$)H$_2$) were generally less soluble than the corresponding magnesium tetrabenzotriazaporphines. Metal-free tetrabenzotriazaporphines were purified by crystallization from toluene, followed by removal of

impurities by sublimation, the residue after sublimation being the required TBTAP(C$_n$)H$_2$. Zinc tetrabenzotriazaporphines could be obtained from reaction of the corresponding metal-free tetrabenzotriazaporphines and anhydrous zinc acetate.

B. Electronic structure of the TBTAP system

Simple PcM species have D_{4h} symmetry, while demetallation leads to the PcH$_2$ species of D_{2h} symmetry. However, in contrast, in the TBTAP species, the metallated complexes at best have twofold symmetry, while the free base species cannot exceed C_s; thus all orbital degeneracies are lifted, for both metallated and free base. The electronic structure of TBTAPC$_1$Mg has been discussed by Solovev et al. (6) using Gouterman's four-orbital model. For the metal-free and main-group metal derivatives, the HOMO-1, HOMO, LUMO, and LUMO + 1 orbitals of the TBTAP(C$_n$) system are $[b_1(\pi)]^2$, $[a_2(\pi)]^2$, $[b_2(\pi^*)]^0$, and $[b_1(\pi^*)]^0$, respectively (with electron occupations noted). Thus the overall electronic structure parallels that of metal-free phthalocyanine.

C. Electrochemistry

The electrochemical properties of phthalocyanine species are well known (7). The electrochemistry of these triazabenzporphine species was briefly studied to investigate how the replacement of one aza bridgehead by a long-chain-linked CH methine bridgehead influences these properties.

(i) TBTAP(C$_n$)H$_2$

Species **5**, $n = 9$, and **11**, $n = 17$, were chosen to study the effect of the length of the alkyl group in the meso position on the electrochemical properties of the unsubstituted benzo TBTAP derivatives. The electrochemistry of species **13** and **14**, $n = 15$, were investigated to monitor the effect of changing the substituents on the benzo position.

Oxidation and reduction of these compounds directly involve the triazaporphine ring system, since the metal centres

are not redox active. Cyclic voltammograms generally show (e.g., Fig. 1*a*) (Table 1) three waves (two reduction (**III,IV**), one oxidation (**I**); **III,IV** are reversible or quasi-reversible, **I** is usually irreversible) diffusion controlled with $i_c = i_a$, and $i \propto v^{1/2}$ (v = scan rate in cyclic voltammogram) and, in addition, two less well-defined and overlapping oxidation waves, **II** and **II'**. The rest potential lies between processes **II'** and **III**.

A rotating disc (RDE) analysis shows that the sum of the limiting current for waves **II** and **II'** corresponds to a one-electron transfer process (Fig. 1*b*) and is equal to the current for process **I**. Thus processes **II** and **II'** (combined) correspond with ring oxidation to the cation radical, $[TBTAP(-1)H_2]^+/TBTAP(-2)H_2$ (using previously defined nomenclature (8)). A differential pulse voltammetry study shows that the redox potentials for waves **II** and **II'** are concentration dependent. At very low concentration, only one differential pulse signal was observed at a potential close to that of wave **II'** (Table 1, Fig. 2). The concentration limit for observing one peak for species **5** and **13** is below 10^{-5} M, and is below 10^{-6} M for species **14**.

The dual wave arises from aggregation, a well-known phenomenon in phthalocyanine derivative chemistry (9). However Beer–Lambert plots for the parent **5** from 8.2×10^{-5} M to 6.6×10^{-7} M at 687 and 647 nm do not show any deviation from linearity, indicating that the parent unoxidized species is not aggregated. Therefore the oxidized species, $[TBTAP(-1)H_2]^+$, must aggregate according to:

[1] $[TBTAP(-1)H_2]^+ + TBTAP(-2)H_2$

$$<= = => \{[TBTAP(-1)H_2]TBTAP(-2)H_2\}^+$$
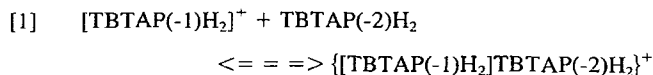
Since it is apparently wave **II'** and not wave **II** which survives in very dilute solution, wave **II'** must correspond to oxidation of the mononuclear species, which then combines, as in eq. [1], to form a mixed valence species that then oxidizes at wave **II** to 2 $[TBTAP(-1)H_2]^+$ (but see below that this species is in equilibrium with a dipositively charged dimeric species). The equilibrium [1] becomes much less important at very low concentrations, as shown in Fig. 2, when only direct oxidation of TBTAP(-2)H_2 to $[TBTAP(-1)-H_2]^+$ is observed. The formation of binuclear mixed-valence single-ring oxidized species such as that shown in eq. [1] is becoming fairly well known in phthalocyanine chemistry, especially with binuclear linked species (10–12), but is also purported to occur (13) during the oxidation of MgPc(-2), via $[MgPc(-1).MgPc(-2)]^+$, to $2[MgPc(-1)]^+$.

Wave **I** is assigned to oxidation to the dication radical, namely, process $[TBTAP(0)H_2]^{2+}/[TBTAP(-1)H_2]^+$. This redox couple is irreversible except for species **14**. Waves **III** and **IV** are quasi-reversible diffusion-controlled one-electron transfer processes assigned to the reduction processes $TBTAP(-2)H_2/[TBTAP(-3)H_2]^-$ and $[TBTAP(-3)H_2]^-/[TBTAP(-4)H_2]^{2-}$, respectively.

Increasing the alkyl chain from 9 to 17 carbon atoms in the *meso* position provides no significant change in the redox potential.

(ii) TBTAP(C_n)Mg (species 4, 10)

These magnesium species show voltammograms typical for MPc-like species with oxidation processes **II** and **I** to the ring-oxidized mono- and di-cation radical, respectively, and two reduction processes (**III, IV**) to the ring-reduced mono- and di-anion radical, respectively (Figs. 3, 4; Table 1). The

forward and reverse differential pulse polarograms are especially well behaved (Fig. 4), showing the electrochemical reversibility of all the observed processes, with the exception of **I** (and possibly **IV**, see below).

(iii) Comparison with regular phthalocyanine species

Although the overall features in the electrochemical behaviour of the TBTAP species parallel those of the phthalocyanines very closely, the first and second reductions for $TBTAP(C_n)H_2$ are about 300 mV negative of those for regular metal-free phthalocyanine species such as metal-free tetraneopentoxyphthalocyanine (6, 14). This is due to the replacement of one electron-withdrawing bridgehead nitrogen link by the less-withdrawing methine link. Porphyrins are more difficult to reduce than the corresponding phthalocyanines and these TBTAP species obviously lie, in character, between the porphyrins and phthalocyanines.

The naphthalene-substituted species, **14**, is easier to oxidize and more difficult to reduce than the corresponding benzotriazaporphin, an observation consistent with previous phthalocyanine experience (7).

D. Electronic absorption

(i) TBTAP(C_n)H_2 and TBTAP(C_n)M

In the electronic spectroscopy of fourfold symmetry, D_{4h}, MPc(-2) species, $\pi-\pi^*$ transitions from the two upper filled π orbitals (HOMO and HOMO-1) to the π^* LUMO orbital provide a strong band, usually in the range 620–720 nm, called the Q band, and a second band, in the range 320–420 nm, called the B band (or Soret). The Q band is usually associated with a weaker vibrational satellite to higher energy (near 600–620 nm) (15). In the metal-free species, of twofold symmetry, the Q band is split into two strong features, usually with at least two weaker vibrational satellites. Such a doubled Q band is expected, and observed, in these lower symmetry TBTAP(-2)(C_n)H_2 and TBTAP(-2)-(C_n)M species (Fig. 5). The data reported here (Table 2) correspond closely with those previously published for TBTAP(-2)H_2, TBTAP(-2)Mg, and TBTAP(-2)Zn (3, 5).

The Q-band splitting in the spectra of the TBTAP(-2)(C_n)M species is about 500 cm^{-1}, whereas it is about 900 cm^{-1} in the spectra of metal-free TBTAP(-2)(C_n)H_2, perhaps because of the lower symmetry of the latter. This Q-band splitting is substantially larger than that imposed on mixed benzo, naphthophthalocyanines where one or three benzene rings is replaced by a napthalene ring; such systems show splittings (16) of 225–250 cm^{-1}. Changing the length of the alkyl chain causes no significant shift or change in the relative intensities of either the Q or B bands, in the spectrum recorded in THF.

(ii) Spectroelectrochemistry

(a) Cation radicals, (a_2)', $^2A_2$: The spectroscopic changes accompanying the oxidation of TBTAP(C_9)Mg (**4**) and *t*-BuTBTAP(C_{15})H_2 (**13**) to their corresponding cation radicals are shown in Figs. 6 and 7. The resulting loss of Q-band intensity between 600 and 700 nm, and the growth of weaker and broader absorption near 550 and 850 nm, is typical of the formation of a phthalocyanine cation radical, Pc(-1), species (13, 17, 18) (Table 3). Indeed the spectra (13, 18) of ZnPc(-1) and MgPc(-1) species are dramatically similar to those spectra reported here, leaving no doubt that these species are cation radicals. The principal difference is that

the band near 850 nm, reputed to be the Q band for the monomeric cation radical (13), is relatively less strong, and is broader, than in the MPc(-1) species. The broadness may reflect incipient splitting in the lower symmetry of these species. The peak at 530–570 nm is a π–π transition in the mononuclear species, similar to previous assignments of related species (13, 14, 18, 20, 21).

These species show isosbestic points upon reduction and may be oxidized back to the starting species with recovery of the initial spectrum; thus the spectroelectrochemistry is reversible with no significant decomposition.

The presence of a hole in the HOMO orbital frequently leads, in phthalocyanine chemistry, to some stabilization of a dimeric species (8, 10–12, 18, 19), which may be written for the TBTAP species as:

[2] $2[\text{TBTAP}(-1)\text{H}_2]^+ <= = => [\text{TBTAP}(-1)\text{H}_2]_2^{2+}$
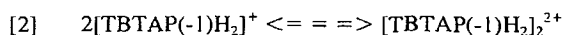
Comparison of the electronic spectra of phthalocyanine and TBTAP cation radical spectra leads to the presumption that the peak at 1010–1080 nm arises from dimeric TBTAP radical cation species. Support for this conclusion arises from concentration-dependent studies that show, for TBTAP-$(\text{C}_{15})\text{H}_2$, that the intensity ratio for the peak at 1070 nm relative to that at 860 nm increases with increasing concentration, e.g., the ratio 1070/860 is 0.4 at 2.5×10^{-4} M, and 1.1 at 1×10^{-3} M TBTAP(-2)H$_2$.

(b) Mono-anion radicals $(a_2)^2(b_2)^1$, $^2B_2$: Figure 8 shows the spectroscopic changes during the reduction of **13** to its anion radical with related data for other species in Table 4. Isosbestic points again attest to good behaviour with no significant decomposition. The spectroscopic features are characteristic of Pc(-3) anion radicals (14, 16, 22–24). While MPc(-2) species yield a single Q band, [MPc(-3)]$^-$ species usually have a doubled band in the Q region. Conversely, these low-symmetry [TBTAP(-3)(C_n)]$^-$ species only exhibit a single band in the Q region (Fig. 8). A magnetic circular dichroism study of these and related systems provides an explanation of this apparent anomaly and will be published elsewhere.[2] Otherwise the spectra are characteristic of the mono-anion radical, especially with respect to the band near 440 nm and the double system (assigned as π^*–π^*) near 860 and 950 nm, which, however, is red shifted from the corresponding bands in the phthalocyanine series (14, 22–24).

(c) Di-anion radicals $(a_2)^2(b_2)^2$ $^1A_1$: The spectroscopic changes during the reduction of the mono-anion radical of **5** to its di-anion radical are shown in Fig. 9, with data for other di-anion radicals summarized in Table 4. The metal-free di-anion radical spectra show clean complete reduction with isosbestic points. However, some decomposition is noted during the reduction of the Mg species to the di-anion state. These spectroscopic data are characteristic for Pc(-4) species, especially the strong band near 530 nm (14); in this case, the number of strong features in the Pc(-4) and TBTAP(-4)(C_n) spectra and the overall shape of the band envelope are similar.

Summary

The spectroscopic and electrochemical properties of the triazaporphine species parallel very closely those for twofold symmetry metallophthalocyanines. The presence of one methine linkage replacing an aza bridgehead does not, it appears, have a major effect upon the electronic properties of these phthalocyanine-like species save for removing all orbital degeneracies. Thus the wealth of understanding that has grown in the phthalocyanine field can be transferred with some confidence to the triazaporphines, subject only to the change in symmetry. These species do have some important properties, however, which make them very useful in the pursuit of molecular electronic applications, namely: *(i)* organic solvent soluble, single isomer, species can readily be synthesized; *(ii)* Langmuir–Blodgett films may readily be made from amphiphilic species constructed with long alkyl chains (25–27); *(iii)* the facile ability to modify the functional group attached to the methine linkage should provide for the synthesis of a wide range of strategically designed molecules.

1. P. A. Barrett, R. P. Linstead, G. A. P. Tuey, and J. M. Robertson. J. Chem. Soc. 1809 (1939).
2. R. L. Wheeler, G. Nagasubramanian, A. J. Bard, L. A. Schectman, D. R. Dininny, and M. E. Kenney. J. Am. Chem. Soc. **106**, 7404 (1984).
3. C. C. Leznoff and N. B. McKeown. J. Org. Chem. **55**, 2186 (1990).
4. T. J. Dougherty, W. R. Potter, and K. R. Weishaupt. *In* Porphyrin localization and treatment of tumors. *Edited by* D. R. Doirin and C. J. Gomer. Alan R. Liss Inc., New York. 1984. p. 301; S. G. Brown, C. J. Tralau, P. D. Coleridge Smith, D. Akademir, and T. Weiman. J. Cancer, **54**, 43 (1986); I. Rosenthal, E. Ben-Hur, S. Greenberg, A. Conception-Lam, D. M. Drew, and C. C. Leznoff. Photochem. Photobiol. **46**, 959 (1987); I. Rosenthal and E. Ben-Hur. *In* Phthalocyanines; properties and applications. Vol. 1. *Edited by* C. C. Leznoff and A. B. P. Lever. VCH Publishers, New York. 1989. p. 393. J. E. Van Lier. Photodynamic therapy of neoplastic disease. Vol. 1. *Edited by* D. Kessel. CRC Press, Boca Raton, Fla. 1990. p. 279; T. J. Dougherty. Photochem. Photobiol. **45**, 897 (1987); B. W. Henderson and T. J. Dougherty. Photochem. Photobiol. **55**, 145 (1992).
5. M. Krejcik, M. Danek, and F. Hartl. J. Electroanal. Chem. **317**, 179, (1991).
6. K. N. Solovev, V. A. Mashenkov, and T. F. Kachura. Opt. Spectrosc. (Engl. Transl.) **27**, 24 (1969).
7. A. B. P. Lever. *In* Phthalocyanines; properties and applications. Vol. 3. *Edited by* C. C. Leznoff and A. B. P. Lever. VCH Publishers, New York. 1993. p. 1.
8. J. F. Myers, G. W. Rayner Canham, and A. B. P. Lever. Inorg. Chem. **14**, 461 (1975).
9. W. A. Nevin, W. Liu, and A. B. P. Lever. Can. J. Chem. **65**, 855 (1986); W. A. Nevin, W. Liu, M. Melnik, and A. B. P. Lever. J. Electroanal. Chem. **213**, 217 (1986); W. A. Nevin, W. Liu, S. Greenberg, M. R. Hempstead, S. M. Marcuccio, M. Melnik, C. C. Leznoff, and A. B. P. Lever. Inorg. Chem. **26**, 891 (1987); Z. A. Schelly, R. D. Farina, and E. M. Eyring. J. Phys. Chem. **74**, 616 (1970); K. Bernauer and S. Fallab. Helv. Chim. Acta, **44**, 1287 (1961); A. Giraudeau, A. Louati, M. Gross, J. J. Andre, J. Simon, C. H. Su, and K. M. Kadish. J. Am. Chem. Soc. **105**, 2917 (1983).
10. V. Manivannan, W. A. Nevin, C. C. Leznoff, and A. B. P. Lever. J. Coord. Chem. **19**, 139 (1988).

[2]N. Kobayashi, A. B. P. Lever, and M. J. Stillman. Manuscript in preparation.

11. N. Kobayashi, H. Lam, W. A. Nevin, P. Janda, C. C. Leznoff, and A. B. P. Lever. Inorg. Chem. **29**, 3415 (1990).
12. C. C. Leznoff, H. Lam, W. A. Nevin, N. Kobayashi, P. Janda, and A. B. P. Lever. Angew. Chem. Int. Ed. Engl. **26**, 1021 (1987).
13. E. Ough, E. Z. Gasyna, and M. J. Stillman. Inorg. Chem. **30**, 2301 (1991).
14. G. Fu, Y. S. Fu, K. Jayaraj, and A. B. P. Lever. Inorg. Chem. **29**, 4090 (1990).
15. M. J. Stillman. *In* Phthalocyanines; properties and applications. Vol. 1. *Edited by* C. C. Leznoff and A. B. P. Lever. VCH Publishers, New York. 1989. p. 133.
16. Y. Ikeda, H. Konami, M. Hatano, and K. Mochizuki. Chem. Lett. 763 (1992).
17. M. J. Stillman. *In* Phthalocyanines: properties and applications. Vol. 3. *Edited by* C. C. Leznoff and A. B. P. Lever. VCH Publishers, New York. 1993. p. 277.
18. T. Nyokong, T. Z. Gasyna, and M. J. Stillman. Inorg. Chem. **26**, 548 (1987).
19. H. Z. Homborg. Z. Anorg. Allg. Chem. **507**, 35 (1983).
20. W. A. Nevin, M. R. Hempstead, W. Liu, C. C. Leznoff, and A. B. P. Lever. Inorg. Chem. **26**, 570 (1987).
21. P. A. Bernstein and A. B. P. Lever. Inorg. Chem. **29**, 608 (1990).
22. P. C. Minor, M. Gouterman, and A. B. P. Lever. Inorg. Chem. **24**, 1894 (1985).
23. D. W. Clack and J. R. Yandle. Inorg. Chem. **11**, 1738 (1972).
24. J. Mack, S. Kirkby, E. A. Ough, and M. J. Stillman. Inorg. Chem. **31**, 1717 (1992).
25. S. Baker, M. C. Petty, G. G. Roberts, G. G. and M. V. Twigg. Thin Solid Films, **99**, 53 (1983); H. Fuchs, H. Ohst, and W. Prass. Adv. Mater. (Weinheim, Fed. Repub. Germany), **3**, 10 (1991); G. G. Roberts, M. C. Petty, S. Baker, M. T. Fowler, and N. J. Thomas. Thin Solid Films, **132**, 113 (1985); M. Sugi. J. Mol. Electron. **1**, 3 (1985); R. H. Tredhold. Rep. Prog. Phys. **50**, 1609 (1987).
26. Y. S. Fu and A. B. P. Lever. J. Phys. Chem. **95**, 6979 (1991).
27. M. J. Cook, N. B. McKeown, A. J. Thomson, K. J. Harrison, R. M. Richardson, A. N. Davies, and S. J. Roser. Chem. Mater. **1**, 287 (1989); J. R. Fryer, C. M. Mcconnell, R. A. Hann, B. L. Eyres, and S. K. Gupta. Philos. Mag. B: **61**, 843 (1990); S. Palacin, A. Ruaudel-Teixier, and A. Barraud. J. Phys. Chem. **93**, 7195 (1989).